Activation of the calcium-sensing receptor in human valvular interstitial cells promotes calcification

Hawraa Issa, Lucie Hénaut, Jeanne Bou Abdallah, Cédric Boudot, Gaëlle Lenglet, Carine Avondo, Aida Ibrik, Thierry Caus, Michel Brazier, Romuald Mentaverri, et al.

Activation of the calcium-sensing receptor in human valvular interstitial cells promotes calcification

Hawraa Issa[1,2], Lucie Hénaut[1], Jeanne Bou Abdallah[1], Cédric Boudot[1], Gaëlle Lenglet [1], Carine Avondo[1], Aida Ibrik[2], Thierry Caus[1,3], Michel Brazier [1,4], Romuald Mentaverri[1,4], Kazem Zibara[2], Saïd Kamel[1,4].

1. EA7517, MP3CV, CURS, University of Picardie Jules Verne, Amiens, France.
2. ER045, PRASE, Biology Department, Faculty of Sciences, Lebanese University, Beirut, Lebanon.
3. Heart, Chest, and Vascular Surgery Center, Amiens University Hospital, Amiens, France.
4. Biochemistry Laboratory, Amiens University Hospital, Amiens, France

Running title: The CaSR in aortic valve calcification

Corresponding authors:
Professor Saïd Kamel
MP3CV, EA7517, CURS
Université Picardie Jules Verne
Chemin du Thil
F-80025 Amiens cedex 1
France
Phone: +33-322-825-425
E-mail: said.kamel@u-picardie.fr

Word count: 6596 (without references)

Total number of figures and tables: 5

Glossary:

αSMA: alpha-smooth muscle actin

Bmp2: bone morphogenetic protein 2

CAVD: calcific aortic valve disease

CaSR: calcium-sensing receptor

HVIC: human aortic valve interstitial cell

Opn: osteopontin

Osx: osterix

Runx2: runt-related transcription factor 2

VSMC: vascular smooth muscle cell

Highlights:

- Human valvular interstitial cells (hVICs) express the calcium-sensing receptor (CaSR)
- CaSR activation promoted the mineralization and osteogenic transition of hVICs.
- CaSR activation reduced the expression of the calcification inhibitor osteopontin
- In hVICs, the CaSR might be a key promoter of calcific aortic valve disease progression.

Abstract

Introduction and aims. Calcific aortic valve disease (CAVD) is the most common heart valve disease in western countries. It has been reported that activation of the calcium-sensing receptor (CaSR) expressed by vascular smooth muscle cells prevents vascular calcification. However, to date, the CaSR's expression and function in cardiac valves have not been studied. The present study sought to evaluate the presence of the CaSR within human valvular interstitial cells (hVICs), assess the CaSR's functionality, and ascertain its involvement in hVIC calcification.

Methods and results. Data from Western blot, flow cytometry and immunocytochemistry experiments demonstrated that primary hVICs express the CaSR. The receptor was functional, since the incubation of hVICs with the calcimimetic R-568 significantly increased Ca^{2+}-induced ERK1/2 phosphorylation, and exposure to the calcilytic NPS2143 reduced ERK1/2 activation. A reduction in endogenous CaSR expression by hVICs (using siRNA) was associated with significantly lower levels of Ca^{2+}-induced mineralization (quantified using Alizarin Red staining). Similar data were obtained after the pharmacological inhibition of CaSR activity by the calcilytic NPS2143. In contrast, overexpression of a functional CaSR amplified Ca^{2+}-induced calcification. Pharmacological activation of the CaSR with the calcimimetic R-568 showed similar effects. CaSR's procalcific properties are associated with increased osteogenic transition (as characterized by elevated mRNA expression of bone morphogenetic protein 2 and osterix), and reduced the expression of the calcification inhibitor osteopontin. Histological analysis of 12 human aortic tricuspid valves showed that CaSR expression was greater in calcified areas than in non-calcified areas. These data were confirmed by Western blots.

Conclusions. To the best of our knowledge, this study is the first to have demonstrated that hVICs express a functional CaSR. Taken as a whole, our data suggest that activation of the CaSR expressed by hVICs might be a key promoter of CAVD progression.

Keywords: calcium-sensing receptor, cardiac valve calcification, valvular interstitial cell.

1. Introduction

Heart valve disease is a major public health problem in industrialized countries [1]. Indeed, calcific aortic valve disease (CAVD), which affects a relatively high proportion of older adults, is the most common heart valve disease in the western world [2,3]. This disease shares a number of risk factors with vascular atherosclerosis, and the very high associated hospitalization rates have prompted the description of CAVD as the “next cardiac epidemic” [4]. Calcific aortic valve disease consists primarily of aortic valve sclerosis, which progresses to end-stage calcific aortic stenosis and is accompanied by the progressive thickening and calcification of the valve leaflets [5]. Systemic cardiovascular effects may then occur, since the progressive leaflet fibrosis and calcification interfere with valve cusp opening, and thus impede left ventricular outflow [6]. Potential CAVD promoters include male sex, smoking, high body mass index, hypertension, elevated blood lipids, a bicuspid aortic valve, type II diabetes mellitus, and end-stage renal disease [7]. There are no pharmacologic treatment options at present, and so the only solution is valve replacement [8]. However, valve replacement is risky in elderly adults, and calcification can develop on the bioprosthetic valves - leading to more severe complications. A better understanding of the pathophysiology of CAVD is thus required for the development of novel therapeutic strategies [9] that would slow the disease progression.

Calcific aortic valve disease was long considered to be a passive degenerative condition. However, it is now conceptualized as a more complex, actively regulated disease process [10] that results from a phenotypic switch of quiescent valvular interstitial cells to a myofibroblast-like phenotype and then an osteoblast-like phenotype [11]. Heart valves contain a heterogeneous population of valvular endothelial cells and valvular interstitial cells (VICs), which maintain valve

homeostasis and leaflet integrity. Valvular interstitial cells (the most abundant cell type in the heart valves) have a key role in CAVD progression. Under physiological conditions, most VICs have a fibroblastic phenotype, produce extracellular matrix proteins, and release the growth factors and cytokines needed to maintain the valve's structure [12]. In calcified aortic valves, however, most of the VICs display a myofibroblast-like phenotype characterized by the expression of high levels of α-smooth muscle actin (α-SMA) and bone morphogenetic protein 2 (Bmp2) [12]. Elevated proliferative activity and the overproduction of extracellular matrix by these VICs lead to aortic valve fibrosis and valvular thickening. It is noteworthy that VICs in calcified valves may also display an osteogenic phenotype, with enhanced expression of osteoblast markers like runt-related transcription factor 2 (Runx2), osterix (Osx), Bmp2, and osteopontin (Opn) [12,13]. The osteoblast-like activity of these VICs is thought to be responsible for the mineralization process associated with CAVD [11,14]. However, the exact cellular and molecular pathways of CAVD initiation and progression remain poorly understood.

Extracellular calcium (Ca^{2+}) is a key inducer of the calcification process [15] and is also an important messenger in the cardiovascular system - particularly via its effects on the calcium-sensing receptor (CaSR) [16]. The CaSR is a member of the G–protein–coupled receptor family; it was initially cloned in parathyroid gland cells, where the receptor is involved in the regulation of parathyroid hormone synthesis and secretion in response to changes in the extracellular ionized calcium concentration [17]. Within the vasculature, the CaSR is known to be expressed by cardiomyocytes [18,19], endothelial cells [20] and vascular smooth muscle cells (VSMCs) [21–23]. Our group recently reported that activation of the CaSRs expressed by VSMCs reduces the development of calcification [24,25]. However, the expression and

function of the CaSR in the cardiac valves have not previously been studied. The present study was designed to evaluate the presence of the CaSR within human valvular interstitial cells, (hVICs), assess the receptor's functionality, and to ascertain its involvement in hVIC calcification.

2. Materials and Methods

2.1. Culture of hVICs

Human aortic tricuspid valves were collected anonymously from patients with CAVD undergoing valve replacement surgery at Amiens Picardie University Hospital (Amiens, France). In accordance with French legislation, the patients gave their informed consent to participation. The study was approved by the local ethics committee (study number: 2009-19). The hVICs were isolated from non-calcified areas of the valves, and were characterized as described previously [26,27]. Dulbecco's Modified Eagle's Medium (DMEM) D6546 (Sigma Aldrich) supplemented with 10% fetal bovine serum (FBS) was used for cell culture. Experiments were performed on cells from passages 2 to 6.

2.2. The hVIC mineralization assay

Mineralization of hVICs (10000 cells per well, in 48-well plates) was induced by 14 days of exposure to 1%-FBS-supplemented DMEM containing either 5.0 mmol/l calcium (the pro-calcific condition) or 1.8 mmol/l calcium (the non-calcific condition). To evaluate the impact of CaSR activity on calcium-induced mineralization, a positive allosteric modulator of the CaSR (the calcimimetic R-568; 0.1 µmol.L; Sigma-Aldrich, St. Louis, MO) or a CaSR inhibitor (the calcilytic NPS2143; 0.1 µmol.L; Tocris Biosciences) was added to the culture medium.Half of the mineralization medium was renewed every two days. Mineral deposition was detected and quantified using Alizarin Red staining. Briefly, samples were fixed (with 50% ethanol for 5 min, and the 95% ethanol for 5 min), stained for 5 min with Alizarin Red S (40 mmol/l, pH 4.2), rinsed with 50% ethanol, and photographed. Alizarin Red was then solubilized by

incubation in buffer containing 10 mmol/l NaH_2PO_3 and 10% hexadecylpyridinium chloride monohydrate, prior to reading at 570 nm.

2.3. Cell viability assay

A methylthiazolyldiphenyl-tetrazolium bromide (MTT, Sigma-Aldrich, St. Louis, MO) assay was used to evaluate the viability of hVICs in response to high Ca^{2+} concentrations and/or CaSR pharmacological modulators. Briefly, hVICs (5000 cells per well in 96-well plates) were cultured for 14 days under non-calcific conditions or pro-calcific conditions in the presence or absence of 0.1 µmol//L of the calcimimetic R-568 or the calcilytic NPS2143. After stimulation, a MTT solution was added to each well (final MTT concentration: 500 µg/ml) and the plates were incubated for 1 h. Formazan crystals formed by living cells were then dissolved in DMSO, and the absorbance was measured at 570 nm.

2.4. RNA extraction and real-time PCR

After experimental treatments, mRNA was extracted from hVICs (200000 cells per well in 6-well plates) using an RNeasy® Mini Kit, according to the manufacturer's specifications (Qiagen). For gene expression analysis, reverse transcription was performed using the High Capacity cDNA Reverse Transcription Kit (Invitrogen). Real-time PCR was performed with the Power SYBR® Green PCR Master Mix (Fisher Scientific) and the following primer sequences: for CaSR (F) 5'-AGGAAAGGGATCATTGAGGG-3' and (R) 5'-ATGCAGGAGGTGTGGTTCTC-3'; for Bmp2 (F) 5'-CGGACTGCGGTCTCCTAA-3' and (R) 5'-GGAAGCAGCAACGCTAGAAG-3'; for Runx2 (F) 5'-GGCCCACAAATCTCAGATCGTT-3' and (R) 5'-CACTGGCGCTGCAACAAGAC-3';

193 for Opn (F) 5'-ATCACCTGTGCCATACCAGTTAAAC-3' and (R) 5'-
194 CCACAGCATCTGGGTATTTG-3'; for Osx (F) 5'-CAAGGTGTATGGCAAGGCTTC-3'
195 & (R) 5'-AGCTCATCCGAACGAGTGAAC-3'; for αSMA (F) 5'-
196 CCAGCAGATGTGGATCAGCA-3' & (R) 5'-AAGCATTTGCGGTGGACAAT-3'; the
197 primer sequences for GAPDH were (F) 5'-TCGGAGTCAACGGATTTGG-3' & (R) 5'-
198 GCAACAATATCCACTTTACCAGAGTTAA-3'. Transcript levels were quantified using
199 CFX Manager™ software (version 3.1, Bio-Rad) and normalized against *GAPDH*
200 expression.
201

202 **2.5. Western blotting**

203 After experimental treatments, hVICs (200000 cells per well, in 6-well plates) were
204 washed with PBS and then homogenized in lysis buffer (25 mM Tris-HCl, 250 mM
205 NaCl, 5 mM EDTA, and 1% SDS, pH 7.4) prepared with phosphatase and protease
206 inhibitor cocktails. The samples were agitated for 30 min and then centrifuged to
207 collect the supernatant. Proteins were assayed using the DC™ Protein Assay Kit
208 (Bio-Rad) and stored at -80°C for later analysis. For the extraction of proteins from
209 valvular tissues, samples were transferred into liquid nitrogen and pulverized with a
210 homogenizer. Protein samples from hVICs and valve tissues were separated using
211 8% SDS-PAGE under reducing conditions. After electrophoresis, samples were
212 transferred to nitrocellulose membranes (reference 10600002, Amersham,). For the
213 Western blots of ERK1/2, samples were blocked with 5% milk prepared in TBS 0.1%
214 Tween for 1 h. For Western blots of CaSR, the blocking solution consisted of 5% milk
215 prepared in PBS 1% Triton X-100. Incubation with rabbit polyclonal anti-
216 phosphorylated ERK (Cell Signaling, Danvers, MA; #9101, 1:1000 dilution), mouse
217 monoclonal anti-CaSR (Novus Biologicals, #NB120-19347, 1:500 dilution) or mouse

monoclonal anti-β-actin (Sigma Aldrich, #A1978, 1:5000 dilution) antibodies was performed overnight at 4 °C. A solution of 5% milk prepared in TBS 0.1% Tween was used to dilute the anti-ERK and -actin primary antibodies, while a solution of 0.5% milk prepared in PBS 1% Triton X-100 was used to dilute the anti-CaSR primary antibody. Blots were washed either with TBS/Tween (for ERK1/2 and β-actin) or PBS 1% Triton X-100 containing 0.5% milk (for CaSR), prior to incubation with an appropriate horseradish-peroxidase-conjugated secondary antibody (Santa Cruz Biotechnology, #sc-2004, #sc-2005, 1:5000). After washing, the blots were developed with chemiluminescence reagents (Bio-Rad). The blots were viewed using the Chemidoc Imaging System (Bio-Rad), and quantified using Image J software. The expression levels were corrected for minor loading differences by normalization against β-actin.

2.6. Transfection with siRNAs

Human VICs were transfected with siRNA diluted in OptiMEM (Gibco, Carlsbad, CA), using siPORTNeoFX (Invitrogen). SiPORTNeoFX was chosen because it allowed to transfect hVICs with siRNAs several times over the calcification process without cytotoxicity. A siRNA targeting the CaSR (Invitrogen) was used at a concentration of 30 nM (sense sequence: CCAUUGGAUUCGCUCUGAAtt / antisense sequence: UUCAGAGCGAAUCCAAUGGtg). Scrambled siRNA (Silencer Select Negative Control #2 siRNA, cat # 4390847, Ambion, Foster City, CA) served as a negative control. For mineralization experiments on transfected hVICs, cells were re-transfected every 4 days during the mineralization test, in order to ensure optimal siRNA activity.

2.7. Plasmid transfection

Wild-type CaSR cDNA (described previously) was used for the transient transfection of hVICs [28]. The coding regions of the Wild-type CaSR gene were amplified by PCR and subcloned into the HindIII/XbaI sites of the pcDNA3.1/Zeo(+) vector (V860-20, Invitrogen). Primary hVICs were transiently transfected with pcDNA3.1/Zeo(+) vector containing CaSR-WT cDNA using Lipofectamine 2000 (Invitrogen, #11668-027). The ratio of DNA (in µg) to Lipofectamine Tm 2000 (in µl) used to prepare the complexes was 1:2. Human VICs transfected with the empty vector (EV) were used as controls. Cells were then routinely treated in DMEM supplemented with 1% FBS and 1% GlutaMax but without penicillin-streptomycin. To evaluate the impact of CaSR activity on the expression of the early markers, the cells were transfected for 3 days only in the presence of 1.8 or 5.0 mmol/L Ca^{2+}. Human VICs couldn't handle several plasmids transfections with Lipofectamine 2000 without increasing cytotoxicity. Therefore, to avoid excessive death during the 14 days of the calcification process, hVICs were transfected only once, at the beginning of the experiment. The overexpression of the WT CaSR during the first 3 days of the calcification process was sufficient to modify hVICs phenotype and to obtain a significant difference in terms of calcification after 14 days of culture.

2.8. CaSR flow cytometry

After experimental treatments, hVICs were detached and permeabilized using the Cytofix/CytopermTM Plus Fixation/Permeabilization kit (BD Biosciences, 554 715), according to the manufacturer's instructions. Cells were then incubated for 1 h at 4°C with primary antibody [mouse monoclonal anti-CaSR antibody (5C10, ADD), Abcam ab19 347; 1:40 dilution of the supplied solution], washed in PBS containing 0.5%

bovine serum albumin (BSA), and labelled using polyclonal goat anti-mouse immunoglobulins/RPE (Dako-Cytomation R0480, 1:50 dilution). Protein expression was assessed by flow cytometry using a FACS Canto II system (BD Biosciences). The results are presented as the percentage of the control condition (1.8 mmol/L Ca^{2+}).

2.9. CaSR immunostaining

We measured the expression of CaSR on hVICs and human valve samples. For the histological analysis of human tissue, aortic valve samples were isolated from 12 different patients. Non-calcified and calcified areas were separated, included in OCT, and cut into 7 µm sections with a cryostat.

To perform CaSR immunostaining, samples were fixed with 2% ice-cold paraformaldehyde for 5 min at room temperature (RT), and permeabilized for 10 min at RT with 0.1% Triton X-100 in PBS containing 1% BSA. Samples were then either quenched in 50 mmol/L NH_4Cl/PBS for an additional 10 min (for CaSR fluorescent detection) or exposed to 0.3% H_2O_2 in PBS 1% BSA for 10 min at RT (to block endogenous peroxidase activity when detecting CaSR with peroxidase reagent). Non-specific antibody binding was blocked by incubation in a blocking solution (1% BSA in PBS) for 30 min at RT. Samples were then incubated overnight at 4°C with the primary anti-CaSR antibody (catalog NB 120-19347, Novus Biotechnology, 1:50 dilution) or the control isotype (catalog X0936, Dako, 1:50 dilution) in PBS with 0.5% BSA. Samples were then rinsed 3 times in PBS with 1% BSA, and incubated for 1 h at RT with the secondary antibody (catalog #A11004, Invitrogen, 1:500 dilution for fluorescent detection or catalog #sc-2005, Santa Cruz Biotechnology, Inc., 1:500 dilution for peroxidase detection). The coverslips were then thoroughly washed in

PBS. For peroxidase detection, samples were incubated with substrate kit for peroxidase (Vector® NovaRED™ SK-4800) at RT until suitable staining developed. Finally, the coverslips were counterstained with hematoxylin solution or Hoechst solution, and mounted on glass microscope slides using VectaMount™ mounting medium (Vector® H-5000) for peroxidase detection or Mowiol solution (Calbiochem®, Mowiol® 4-88) for fluorescent detection). Sections were examined with the Zeiss AxioImager D2 laser fluorescence microscope (Microvision).

2.10. Alizarin Red staining on tissue sections

Briefly, tissue sections were incubated in Alizarin Red S solution (40 mmol/l, pH 4.2) for 2 min. Excess dye was removed, and the sections were dehydrated in 100% acetone for 1 min and then in acetone-toluene solutions for 1 min. Lastly, sections were cleared for 5 min in toluene and mounted using DPX Mountant for histology (Sigma-Aldrich).

2.11. Statistical analysis

The results represent at least three independent experiments (i.e. using cells isolated from three different donors) performed in triplicate. The data were quoted as the mean ± standard error of the mean (SEM). Statistical analysis was performed using GraphPad Prism software (version 6.01, GraphPad Software Inc., San Diego, CA). Differences between two groups were assessed with an unpaired Student's t-test, and differences between three or more groups were assessed using a one-way analysis of variance with Tukey's post-test. The threshold for statistical significance was set to $p<0.05$.

3. Results

3.1. Functional calcium-sensing receptor is expressed by human VICs

Data from our immunocytochemistry and flow cytometry experiments demonstrated that the CaSR is expressed in primary hVICs isolated from human aortic tricuspid valves (Figure 1.A and B). Western blot analysis confirmed the presence of the CaSR in those cells, with one band at approximately 120 kDa (corresponding to the non-glycosylated form) and two bands at approximately 130-140 kDa and 150-160 kDa (corresponding to the immature and mature glycosylated forms of the CaSR, respectively) (Figure 1.C) [29]. In various cell types (including VSMCs, cardiomyocytes and embryonic kidney cells), stimulation of the CaSR results in activation of the ERK1/2 pathway [19,22,30,31]. We therefore investigated the CaSR's functionality in hVICs and the receptor's involvement in Ca^{2+}-induced ERK1/2 phosphorylation. In the hVIC model, exposure to 5 mmol/L of Ca^{2+} was associated with a significant increase in ERK1/2 phosphorylation, which peaked after 15 to 30 min (Supplementary Figure 1). Blockade of CaSR activation by the calcilytic NPS2143 decreased Ca^{2+}-induced ERK1/2 phosphorylation by around a fifth (Figure 1.D). In contrast, stimulation of hVICs with the CaSR co-agonist R-568 significantly increased (by a fifth) Ca^{2+}-induced ERK1/2 phosphorylation (Figure 1.E).

3.2. High Ca^{2+} promotes the osteogenic transition and calcification of hVICs

Experiments with Alizarin Red S staining showed that in our hVIC model, 14 days of exposure to increasing Ca^{2+} concentrations (1.8, 3.0 and 5.0 mmol.L) promoted cell calcification in a concentration-dependent manner (Figure 2.A). To better understand the mechanisms by which high Ca^{2+} induced hVIC calcification, we investigated the medium's impact on the osteoblastic differentiation of hVICs. The

results of qRT-PCR assays showed that one day of exposure to 5 mmol/L Ca^{2+} induced a significant increase in the expression of the osteogenic markers Bmp2, Runx2 and Opn (Figure 2. B, C. and D), which therefore appear to be early markers of the Ca^{2+}-induced osteogenic transition of hVICs. The effect of calcium on Bmp2 and Runx2 was significant throughout the 14 days of the calcification process (Figure 2. B. and C.), whereas Opn expression levels had returned to much the same values as control cells after 14 days of exposure to Ca^{2+} (Figure 2.D). After 14 days, we also observed a significant increase in levels of the osteogenic marker Osx (Figure 2.E), and a significant decrease in expression of the myofibroblast marker α-SMA (Figure 2.F). Since these two transcripts were not modulated after a single day of exposure to high-Ca^{2+}, they appear to be late markers of the Ca^{2+}-induced ostegenic transition in our hVIC model.

3.3. Overexpression of a functional wild-type CaSR amplifies Ca^{2+}-induced hVIC calcification

To investigate the CaSR's role in Ca^{2+}-induced hVIC calcification, cells were transiently transfected with either plasmids containing a full-length wild-type CaSR (CaSR-WT) or empty pcDNA™3.1/Zeo(+) plasmids (Empty Vector (EV)). The transfection efficiency was confirmed by flow cytometry and immunocytochemistry after transfecting hVICs with a CaSR-WT-GFP plasmid (Supplementary Figure 2.A and B). Western blot analyses with an anti-CaSR antibody demonstrated that CaSR-WT-transfected hVICs expressed greater levels of CaSR (by 50%) than EV-transfected cells did (Supplementary Figure 2.C). This effect was confirmed by the immunocytochemical analysis of CaSR expression (Supplementary Figure 2.D). Under pro-calcific conditions, mineral deposition was significantly greater in CaSR-

WT-transfected hVICs than in EV-transfected cells (Figure 3.A). The latter effect was associated with a significant increase in the expression of the osteogenic marker Bmp2 and lower expression of Opn - a factor known to inhibit calcification (Figure 3.B and C.).

3.4. Downregulation of endogenous CaSR expression decreases hVIC calcification

To better characterize the CaSR's involvement in hVIC mineralization, and to discriminate between CaSR-mediated and CaSR-independent Ca^{2+} effects (e.g. those occurring through ion channels), CaSR expression was targeted using a siRNA approach. Three days after transfection, endogenous CaSR expression was 40% lower in hVICs transfected with a siRNA targeting the CaSR (CaSR-siRNA) than in scrambled-transfected cells (Supplementary Figure 3 A. and B). In our model, hVICs were transfected every three days in order to maintain a low level of CaSR expression throughout the mineralization process (Supplementary Figure 3.C, D and E). Alizarin Red staining experiments demonstrated that transfection with the CaSR-siRNA significantly decreased Ca^{2+}-induced mineral deposition in hVICs (about 3-fold), relative to scrambled siRNA-transfected cells (Figure 3.D). A second siRNA targeting CaSR expression was used to confirm these data (Supplementary Figure 4). This effect was associated with a significant increase in Opn expression in CaSR-siRNA-transfected hVICs, relative to scrambled-transfected cells (Figure 3.F). Under these culture conditions, CaSR downregulation did not modulate Bpm2 expression (Figure 3.E).

3.5. Pharmacological modulation of the endogenous CaSR in hVICs dramatically impacts high-Ca^{2+}-induced calcification.

To confirm the data obtained after up- or down-regulation of the CaSR, we next sought to evaluate whether pharmacological modulation of the CaSR by its co-agonists (calcimimetics) or antagonists (calcilytics) could affect the calcification process. To this end, hVICs were incubated for 14 days in pro-calcific condition (5 mmol/L) alone or supplemented with increasing concentrations of either the calcimimetic R-568 (0.1, 0.5 and 1 µmol/L) or the calcilytic NPS2143 (0.001, 0.01 or 0.1 µmol/L). Exposure to the calcimimetic R-568 was associated with a concentration-dependent increase in Ca^{2+}-induced hVIC mineralization (Figure 4.A). It is noteworthy that the lowest concentration of R-568 (0.1 µmol/L) promoted a 3-fold increase in Ca^{2+}-induced hVIC mineralization. Hence, this concentration was used in all subsequent experiments involving R-568. An early decrease in Opn expression was observed (using qRT-PCR) one day after exposure to 0.1 µmol/L R-568 in pro-calcific condition (Figure 4.C). The expression of the early osteogenic marker Bmp2 was not modulated by the calcimimetic under these culture conditions (Figure 4.B). However, in hVICs exposed to pro-calcific conditions for 14 days, the expression of Osx (identified as a late osteogenic marker in this model) was significantly increased in response to the calcimimetic (Supplementary Figure 5.A).

In contrast, exposure to 0.1 µm of the calcilytic NPS2143 induced a significant, 2.5-fold decrease in hVIC mineralization (Figure 4.D). This effect was associated with an early decrease in Bmp2 expression (Figure 4.E). Confirming this observation, Osx levels were significantly lower in hVICs exposed to the calcilytic in pro-calcific conditions for 14 days (Supplementary Figure 5.B). The expression of Opn was not

415 modulated by the calcilytic (Figure 4.F). It should be noted that none of these
416 treatments affected cell viability (Supplementary Figure 6).
417
418 **3.6. CaSR expression is elevated in calcified human aortic tricuspid**
419 **valves.**
420 To better assess the CaSR's role in CAVD, expression of the receptor was
421 measured in 12 human aortic tricuspid valves. A histological analysis demonstrated
422 that in a given patient, CaSR expression was higher in calcified areas of the valve
423 leaflets than in non-calcified areas ("C" and "NC", respectively, in Figure 5.A). This
424 observation was confirmed by a Western blot analysis, which showed a significant
425 more intense CaSR bands in protein samples extracted from calcified aortic tricuspid
426 valves than in samples from non-calcified aortic tricuspid valves (Figure 5.B and C).
427

4. Discussion

Since the presence of the CaSR within the cardiovascular system was demonstrated, several investigators have suggested that local activation of this receptor might modulate the development and progression of cardiovascular disease. In the heart, the CaSR has been reported to be expressed in cardiac fibroblasts and myocytes, where it contributes to normal cardiac function and composition of extracellular matrix [18] . Within the vasculature, the CaSR expressed by endothelial cells participates in vasorelaxation by increasing nitric oxide production [20,32]. It is noteworthy that the CaSR is also expressed in VSMCs [21–23,33]. Indeed, CaSR activation reportedly delay the mineralization process in the latter cells [22,24]. The present study is, we believe, the first to have demonstrated the expression of a functional CaSR in hVICs. We found that the siRNA-induced reduction in endogenous CaSR expression in hVICs was associated with significantly less high-Ca^{2+}-induced osteogenic transition and calcification. Similar data were obtained following the pharmacological inhibition of CaSR activity with the calcilytic NPS2143. In contrast, overexpression of a functional CaSR amplified Ca^{2+}-induced osteogenic transition and calcification. Again, similar data were obtained by the pharmacological activation of the CaSR with the calcimimetic R-568. Taken as a whole, our data suggest that activation of the CaSR in hVICs may be a key driver of CAVD.

In our hVIC model, Bmp2, Runx2, and Opn appeared to be early markers of Ca^{2+}-induced cell calcification, while Osx and α-SMA appeared to be late markers. Overexpression of the CaSR-WT in hVICs almost doubled Bmp2 expression (confirming the importance of CaSR activation in the Ca^{2+}-induced hVIC osteogenic transition), while the blockade of CaSR activity with the calcilytic was associated with a statistically significant, three-fold decrease in the expression of Bmp2. In support of

453 this observation, CaSR activation with the calcimimetic R-568 significantly increased
454 the expression of the osteoblast-specific transcription factor Osx [34,35], while CaSR
455 inhibition with the calcilytic NPS2143 decreased Osx expression by a factor of two. In
456 our model, neither siRNA targeting of CaSR nor exposure to the calcimimetic R-568
457 modulated Bmp2 levels. It is known that activation of the CaSR by different ligands
458 may stabilize the receptor in unique activation states, allowing the preferential
459 stimulation of different signaling pathways. This phenomenon is common in G-
460 protein-coupled receptors, and is referred to as “ligand-biased signaling” [36]. In this
461 context, our group reported that Ca^{2+}-induced CaSR activation promoted osteoclasts
462 apoptosis following phospholipase C activation and NF-κB translocation, whereas
463 strontium-induced CaSR activation promoted osteoclast apoptosis after protein
464 kinase C activation [37]. Orthosteric CaSR modulators (such as Ca^{2+}) bind to the
465 CaSR’s orthosteric fixation site, which is located in the extracellular domain. In
466 contrast, the allosteric modulators (like calcimimetics) bind outside the orthosteric site
467 [38]. Their binding changes the CaSR’s three-dimensional conformation, which in
468 turn modulates the receptor’s affinity for orthosteric CaSR modulators. Interestingly,
469 R-568 and NPS2143 are both known to promote biased signaling at the CaSR
470 [39,40]. In this context, we cannot rule out the possibility that binding of the
471 calcimimetic R-568 to the CaSR expressed by hVICs in our study may have induced
472 a ligand-biased signaling by stabilizing the receptor in a conformation that promoted
473 the osteogenic transition of hVICs through a Bmp2-independent pathway. However,
474 we do not know why Bmp2 was not modulated in CaSR-siRNA transfected cells.
475
476 Osteopontin is best known as an inhibitor of vascular calcification [41,42].
477 Levels of the dephosphorylated, inactive form of Opn are correlated with more severe

calcification in patients with CAVD [43]. In the present work, Opn expression was 4-fold lower in response to either CaSR overexpression or CaSR activation by the calcimimetic R-568. This finding was confirmed by the statistically significant doubling of Opn expression upon transfection of hVICs with a siRNA targeting the CaSR. Taken as a whole, these data suggest that CaSR activation may indirectly favor hVIC calcification by inhibiting the release of the calcification inhibitor Opn. However, the exposure of hVICs to the calcilytic NPS2143 in our study did not modulate Opn expression. Again, it is possible that NPS2143's binding to the CaSR may have induced a ligand-biased signaling by stabilizing the receptor in a conformation that inhibited hVIC calcification through an Opn-independent pathway.

As explained above in the Methods section, the hVICs used in this study were isolated from the non-calcified pieces of human aortic tricuspid valves that had been collected during valve replacement surgery. Since these cells were extracted from a generally disease valve, most of them displayed a myofibroblast-like phenotype at the start of the cell culture, as demonstrated by their high baseline level of αSMA expression (Supplementary Figure 7). This constituted a study limitation, and made it impossible for us to assess the CaSR's role in the early transformation of hVICs into myofibroblasts. For this reason, we focused on the impact of CaSR activation on the hVICs' phenotypic transition from myofibroblast-like cells to osteoblast-like cells. Future studies of hVICs isolated from normal/healthy valves will have to address the effect of CaSR activation on the transformation of hVICs into myofibroblast-like cells.

Most of the *in vitro* and *in vivo* literature data have evidenced CaSR's protective effect against vascular calcification. Indeed, calcimimetic stimulation of the

503 CaSR in VSMCs delayed both Pi- and Ca^{2+}-induced mineralization processes in *in*
504 *vitro* studies [22,24,44]. In particular, CaSR activation protects VSMCs from the
505 osteogenic transition and collagen secretion, and can favor synthesis of the matrix
506 Gla protein [24,45]. In animal models, calcimimetics were even able to prevent
507 vascular calcification in the absence of changes in the serum parathyroid hormone
508 level [46]. Given the calcimimetics' systemic effects on the reduction in the Ca x P
509 product and their local inhibition of VSMC mineralization, it was predicted that the
510 clinical use of these compounds would slow the progression of vascular calcification
511 in patients suffering from chronic kidney disease. To address this hypothesis, the
512 ADVANCE study assessed the progression of vascular and cardiac valve
513 calcifications in hemodialysis patients with secondary hyperparathyroidism in
514 response to the calcimimetic cinacalcet-HCl. Although the ADVANCE trial's results
515 tended to show that cinacalcet slowed down the progression of valve calcification
516 [47–49], an unadjusted intention-to-treat analysis of the EVOLVE study data showed
517 that treatment with cinacalcet did not significantly reduce the risk of death or major
518 cardiovascular events in dialyzed patients with moderate-to-severe secondary
519 hyperparathyroidism [50,51]. In the present study, we demonstrated that activation of
520 the CaSR expressed by hVICs directly promotes the calcification process. It is
521 therefore plausible that because cinacalcet regulates the Ca x Pi product by
522 increasing the CaSR's sensitivity to Ca^{2+} in parathyroid tissue, the calcimimetic might
523 have activated the CaSR expressed by hVICs and thus promoted their calcification.
524
525 The behavior of valvular cells has often been compared to that of vascular
526 cells, in view of the anatomic proximity of these two physiological systems [52].
527 However, recent studies have suggested that valvular cells have more complex,

528 unique behaviors than vascular cells [53–56]. In line with this hypothesis, human
529 VSMCs exposed to an osteogenic environment expressed higher levels of
530 osteogenic markers and displayed greater matrix remodeling than hVICs from same
531 patient [52]. These data suggest the existence of cell-mediated differences between
532 vascular and valvular calcification processes, which may account for the opposite
533 calcification responses of hVICs and VSMCs following CaSR activation.
534
535 Previous studies of VSMCs have reported that the development of *in vitro*
536 calcification is associated with a significant decrease in CaSR expression [22,24].
537 Furthermore, CaSR expression is lower in the aortic tissue of patients with chronic
538 kidney disease (a population prone to arterial calcification) than in healthy subjects
539 [23]. Given the local protective effects reported after activation of the CaSR
540 expressed by VSMCs, it was initially suggested that the reduction in CaSR
541 expression in calcified vessels accounted for the development of vascular
542 calcification. In contrast, CaSR expression in the present work was seen to be higher
543 in the calcified areas of aortic valves than in the non-calcified areas. It remains to be
544 seen whether this elevated CaSR expression results from hydroxyapatite deposition
545 or, conversely, represents an early calcification-promoting event.
546
547 **5. Conclusions**
548 The present study is - to the best of our knowledge – the first to have demonstrated
549 that hVICs express a functional CaSR, the activation of which leads to an accelerated
550 Ca^{2+}-induced osteogenic transition and subsequent calcification. The inhibition of the
551 calcification inhibitor Opn observed after CaSR activation may account for these pro-
552 calcific properties. In this context, targeting hVICs' CaSR activity with

pharmacological inhibitors (such as calcilytics) might be a promising strategy for preventing the development of CAVD in patients with normal renal function.

Acknowledgments

We thank the staff at the Plateforme d'imagerie cellulaire et d'analyse des proteines (ICAP, University of Picardie Jules Verne, Amiens, France) for performing the flow cytometry analyses. We also thank Sabrina Poirot-Leclercq for technical assistance during the reviewing process.

Sources of funding

This research was funded by the Fédérations Hospitalo-Universitaire Amiens Caen Rouen. HI received a doctoral fellowship from the Lebanese "*Association de Spécialisation et d'Orientation Scientifique*" (ASOS). This work was also funded by the French National Research Agency as part of the French government's "Investissements d'Avenir" program (reference: ANR-16-RHUS-0003_STOP-AS).

Disclosure

The authors declare no conflicts of interest regarding the present work.

References

[1] V.T. Nkomo, J.M. Gardin, T.N. Skelton, J.S. Gottdiener, C.G. Scott, M. Enriquez-Sarano, Burden of valvular heart diseases: a population-based study, Lancet. 368 (2006) 1005–1011. doi:10.1016/S0140-6736(06)69208-8.

[2] D. Messika-Zeitoun, L.F. Bielak, P.A. Peyser, P.F. Sheedy, S.T. Turner, V.T. Nkomo, J.F. Breen, J. Maalouf, C. Scott, A.J. Tajik, M. Enriquez-Sarano, Aortic valve calcification: determinants and progression in the population, Arterioscler. Thromb. Vasc. Biol. 27 (2007) 642–648. doi:10.1161/01.ATV.0000255952.47980.c2.

[3] E.R. Mohler, Mechanisms of aortic valve calcification, Am. J. Cardiol. 94 (2004) 1396–1402, A6. doi:10.1016/j.amjcard.2004.08.013.

[4] S. Coffey, B.J. Cairns, B. Iung, The modern epidemiology of heart valve disease, Heart. 102 (2016) 75–85. doi:10.1136/heartjnl-2014-307020.

[5] N.M. Rajamannan, F.J. Evans, E. Aikawa, K.J. Grande-Allen, L.L. Demer, D.D. Heistad, C.A. Simmons, K.S. Masters, P. Mathieu, K.D. O'Brien, F.J. Schoen, D.A. Towler, A.P. Yoganathan, C.M. Otto, Calcific aortic valve disease: not simply a degenerative process: A review and agenda for research from the National Heart and Lung and Blood Institute Aortic Stenosis Working Group. Executive summary: Calcific aortic valve disease-2011 update, Circulation. 124 (2011) 1783–1791. doi:10.1161/CIRCULATIONAHA.110.006767.

[6] C.M. Otto, Valvular aortic stenosis: disease severity and timing of intervention, J. Am. Coll. Cardiol. 47 (2006) 2141–2151. doi:10.1016/j.jacc.2006.03.002.

[7] K.D. O'Brien, Pathogenesis of calcific aortic valve disease: a disease process comes of age (and a good deal more), Arterioscler. Thromb. Vasc. Biol. 26 (2006) 1721–1728. doi:10.1161/01.ATV.0000227513.13697.ac.

[8] M.R. Dweck, N.A. Boon, D.E. Newby, Calcific aortic stenosis: a disease of the valve and the myocardium, J. Am. Coll. Cardiol. 60 (2012) 1854–1863. doi:10.1016/j.jacc.2012.02.093.

[9] J.A. Leopold, Cellular mechanisms of aortic valve calcification, Circ Cardiovasc Interv. 5 (2012) 605–614. doi:10.1161/CIRCINTERVENTIONS.112.971028.

[10] T.A. Pawade, D.E. Newby, M.R. Dweck, Calcification in Aortic Stenosis: The Skeleton Key, J. Am. Coll. Cardiol. 66 (2015) 561–577. doi:10.1016/j.jacc.2015.05.066.

[11] S.H. Lee, J.-H. Choi, Involvement of Immune Cell Network in Aortic Valve Stenosis: Communication between Valvular Interstitial Cells and Immune Cells, Immune Netw. 16 (2016) 26–32. doi:10.4110/in.2016.16.1.26.

[12] A.C. Liu, V.R. Joag, A.I. Gotlieb, The emerging role of valve interstitial cell phenotypes in regulating heart valve pathobiology, Am. J. Pathol. 171 (2007) 1407–1418. doi:10.2353/ajpath.2007.070251.

[13] R. Song, D.A. Fullerton, L. Ao, K.-S. Zhao, T.B. Reece, J.C. Cleveland, X. Meng, Altered MicroRNA Expression Is Responsible for the Pro-Osteogenic Phenotype of Interstitial Cells in Calcified Human Aortic Valves, J Am Heart Assoc. 6 (2017). doi:10.1161/JAHA.116.005364.

[14] K.I. Boström, N.M. Rajamannan, D.A. Towler, The regulation of valvular and vascular sclerosis by osteogenic morphogens, Circ. Res. 109 (2011) 564–577. doi:10.1161/CIRCRESAHA.110.234278.

[15] C.M. Shanahan, M.H. Crouthamel, A. Kapustin, C.M. Giachelli, Arterial calcification in chronic kidney disease: key roles for calcium and phosphate, Circ. Res. 109 (2011) 697–711. doi:10.1161/CIRCRESAHA.110.234914.

621 [16] S. Smajilovic, J. Tfelt-Hansen, Calcium acts as a first messenger through the
622 calcium-sensing receptor in the cardiovascular system, Cardiovasc. Res. 75
623 (2007) 457–467. doi:10.1016/j.cardiores.2007.03.015.
624 [17] E.M. Brown, G. Gamba, D. Riccardi, M. Lombardi, R. Butters, O. Kifor, A. Sun,
625 M.A. Hediger, J. Lytton, S.C. Hebert, Cloning and characterization of an
626 extracellular Ca(2+)-sensing receptor from bovine parathyroid, Nature. 366
627 (1993) 575–580. doi:10.1038/366575a0.
628 [18] R. Schreckenberg, K.-D. Schlüter, Calcium sensing receptor expression and
629 signalling in cardiovascular physiology and disease, Vascul. Pharmacol. (2018).
630 doi:10.1016/j.vph.2018.02.007.
631 [19] J. Tfelt-Hansen, J.L. Hansen, S. Smajilovic, E.F. Terwilliger, S. Haunso, S.P.
632 Sheikh, Calcium receptor is functionally expressed in rat neonatal ventricular
633 cardiomyocytes, Am. J. Physiol. Heart Circ. Physiol. 290 (2006) H1165-1171.
634 doi:10.1152/ajpheart.00821.2005.
635 [20] R.C. Ziegelstein, Y. Xiong, C. He, Q. Hu, Expression of a functional extracellular
636 calcium-sensing receptor in human aortic endothelial cells, Biochem. Biophys.
637 Res. Commun. 342 (2006) 153–163. doi:10.1016/j.bbrc.2006.01.135.
638 [21] S. Smajilovic, J.L. Hansen, T.E.H. Christoffersen, E. Lewin, S.P. Sheikh, E.F.
639 Terwilliger, E.M. Brown, S. Haunso, J. Tfelt-Hansen, Extracellular calcium
640 sensing in rat aortic vascular smooth muscle cells, Biochem. Biophys. Res.
641 Commun. 348 (2006) 1215–1223. doi:10.1016/j.bbrc.2006.07.192.
642 [22] M. Alam, J.P. Kirton, F.L. Wilkinson, E. Towers, S. Sinha, M. Rouhi, T.N. Vizard,
643 A.P. Sage, D. Martin, D.T. Ward, M.Y. Alexander, D. Riccardi, A.E. Canfield,
644 Calcification is associated with loss of functional calcium-sensing receptor in

vascular smooth muscle cells, Cardiovasc. Res. 81 (2009) 260–268. doi:10.1093/cvr/cvn279.

[23] G. Molostvov, S. James, S. Fletcher, J. Bennett, H. Lehnert, R. Bland, D. Zehnder, Extracellular calcium-sensing receptor is functionally expressed in human artery, Am. J. Physiol. Renal Physiol. 293 (2007) F946-955. doi:10.1152/ajprenal.00474.2006.

[24] L. Hénaut, C. Boudot, Z.A. Massy, I. Lopez-Fernandez, S. Dupont, A. Mary, T.B. Drüeke, S. Kamel, M. Brazier, R. Mentaverri, Calcimimetics increase CaSR expression and reduce mineralization in vascular smooth muscle cells: mechanisms of action, Cardiovasc. Res. 101 (2014) 256–265. doi:10.1093/cvr/cvt249.

[25] A. Mary, L. Hénaut, C. Boudot, I. Six, M. Brazier, Z.A. Massy, T.B. Drüeke, S. Kamel, R. Mentaverri. Calcitriol prevents in vitro vascular smooth muscle cell mineralization by regulating calcium-sensing receptor expression, Endocrinology. 156 (2015) 1965–74. doi:10.1210/en.2014-1744.

[26] N. Latif, A. Quillon, P. Sarathchandra, A. McCormack, A. Lozanoski, M.H. Yacoub, A.H. Chester, Modulation of human valve interstitial cell phenotype and function using a fibroblast growth factor 2 formulation, PLoS ONE. 10 (2015) e0127844. doi:10.1371/journal.pone.0127844.

[27] E. Nagy, P. Eriksson, M. Yousry, K. Caidahl, E. Ingelsson, G.K. Hansson, A. Franco-Cereceda, M. Bäck, Valvular osteoclasts in calcification and aortic valve stenosis severity, Int. J. Cardiol. 168 (2013) 2264–2271. doi:10.1016/j.ijcard.2013.01.207.

[28] C. Boudot, L. Hénaut, U. Thiem, S. Geraci, M. Galante, P. Saldanha, Z. Saidak, I. Six, P. Clézardin, S. Kamel, R. Mentaverri, Overexpression of a functional

calcium-sensing receptor dramatically increases osteolytic potential of MDA-MB-231 cells in a mouse model of bone metastasis through epiregulin-mediated osteoprotegerin downregulation, Oncotarget. 8 (2017) 56460–56472. doi:10.18632/oncotarget.16999.

[29] M. Bai, S. Quinn, S. Trivedi, O. Kifor, S.H. Pearce, M.R. Pollak, K. Krapcho, S.C. Hebert, E.M. Brown, Expression and characterization of inactivating and activating mutations in the human Ca2+o-sensing receptor, J. Biol. Chem. 271 (1996) 19537–19545.

[30] O. Kifor, R.J. MacLeod, R. Diaz, M. Bai, T. Yamaguchi, T. Yao, I. Kifor, E.M. Brown, Regulation of MAP kinase by calcium-sensing receptor in bovine parathyroid and CaR-transfected HEK293 cells, Am. J. Physiol. Renal Physiol. 280 (2001) F291-302. doi:10.1152/ajprenal.2001.280.2.F291.

[31] J. Tfelt-Hansen, R.J. MacLeod, N. Chattopadhyay, S. Yano, S. Quinn, X. Ren, E.F. Terwilliger, P. Schwarz, E.M. Brown, Calcium-sensing receptor stimulates PTHrP release by pathways dependent on PKC, p38 MAPK, JNK, and ERK1/2 in H-500 cells, Am. J. Physiol. Endocrinol. Metab. 285 (2003) E329-337. doi:10.1152/ajpendo.00489.2002.

[32] H.Z.E. Greenberg, J. Shi, K.S. Jahan, M.C. Martinucci, S.J. Gilbert, W.-S. Vanessa Ho, A.P. Albert, Stimulation of calcium-sensing receptors induces endothelium-dependent vasorelaxations via nitric oxide production and activation of IKCa channels, Vascul. Pharmacol. 80 (2016) 75–84. doi:10.1016/j.vph.2016.01.001.

[33] J.S. Lindberg, B. Culleton, G. Wong, M.F. Borah, R.V. Clark, W.B. Shapiro, S.D. Roger, F.E. Husserl, P.S. Klassen, M.D. Guo, M.B. Albizem, J.W. Coburn, Cinacalcet HCl, an oral calcimimetic agent for the treatment of secondary

hyperparathyroidism in hemodialysis and peritoneal dialysis: a randomized, double-blind, multicenter study, J. Am. Soc. Nephrol. 16 (2005) 800–807. doi:10.1681/ASN.2004060512.

[34] Y.-J. Kim, H.-N. Kim, E.-K. Park, B.-H. Lee, H.-M. Ryoo, S.-Y. Kim, I.-S. Kim, J.L. Stein, J.B. Lian, G.S. Stein, A.J. van Wijnen, J.-Y. Choi, The bone-related Zn finger transcription factor Osterix promotes proliferation of mesenchymal cells, Gene. 366 (2006) 145–151. doi:10.1016/j.gene.2005.08.021.

[35] K. Nakashima, X. Zhou, G. Kunkel, Z. Zhang, J.M. Deng, R.R. Behringer, B. de Crombrugghe, The novel zinc finger-containing transcription factor osterix is required for osteoblast differentiation and bone formation, Cell. 108 (2002) 17–29.

[36] T. Kenakin, Functional selectivity and biased receptor signaling, J. Pharmacol. Exp. Ther. 336 (2011) 296–302. doi:10.1124/jpet.110.173948.

[37] A.S. Hurtel-Lemaire, R. Mentaverri, A. Caudrillier, F. Cournarie, A. Wattel, S. Kamel, E.F. Terwilliger, E.M. Brown, M. Brazier, The calcium-sensing receptor is involved in strontium ranelate-induced osteoclast apoptosis. New insights into the associated signaling pathways, J. Biol. Chem. 284 (2009) 575–584. doi:10.1074/jbc.M801668200.

[38] Z.A. Massy, L. Hénaut, T.E. Larsson, M.G. Vervloet, Calcium-sensing receptor activation in chronic kidney disease: effects beyond parathyroid hormone control, Semin. Nephrol. 34 (2014) 648–659. doi:10.1016/j.semnephrol.2014.10.001.

[39] A.E. Davey, K. Leach, C. Valant, A.D. Conigrave, P.M. Sexton, A. Christopoulos. Positive and negative allosteric modulators promote biased

719 signaling at the calcium-sensing receptor. Endocrinology. 153 (2012) 1232-41.
720 doi: 10.1210/en.2011-1426.
721 [40] K. Leach, P.M. Sexton, A. Christopoulos, A.D. Conigrave. Engendering biased
722 signalling from the calcium-sensing receptor for the pharmacotherapy of diverse
723 disorders. Br J Pharmacol. 171 (2014) 1142-55. doi: 10.1111/bph.12420.
724 [41] R. Ohri, E. Tung, R. Rajachar, C.M. Giachelli, Mitigation of ectopic calcification
725 in osteopontin-deficient mice by exogenous osteopontin, Calcif. Tissue Int. 76
726 (2005) 307–315. doi:10.1007/s00223-004-0071-7.
727 [42] S.A. Steitz, M.Y. Speer, M.D. McKee, L. Liaw, M. Almeida, H. Yang, C.M.
728 Giachelli, Osteopontin inhibits mineral deposition and promotes regression of
729 ectopic calcification, Am. J. Pathol. 161 (2002) 2035–2046. doi:10.1016/S0002-
730 9440(10)64482-3.
731 [43] R. Sainger, J.B. Grau, P. Poggio, E. Branchetti, J.E. Bavaria, J.H. Gorman, R.C.
732 Gorman, G. Ferrari, Dephosphorylation of circulating human osteopontin
733 correlates with severe valvular calcification in patients with calcific aortic valve
734 disease, Biomarkers. 17 (2012) 111–118. doi:10.3109/1354750X.2011.642407.
735 [44] F.J. Mendoza, J. Martinez-Moreno, Y. Almaden, M.E. Rodriguez-Ortiz, I. Lopez,
736 J.C. Estepa, C. Henley, M. Rodriguez, E. Aguilera-Tejero, Effect of calcium and
737 the calcimimetic AMG 641 on matrix-Gla protein in vascular smooth muscle
738 cells, Calcif. Tissue Int. 88 (2011) 169–178. doi:10.1007/s00223-010-9442-4.
739 [45] P. Ciceri, F. Elli, I. Brenna, E. Volpi, D. Brancaccio, M. Cozzolino, The
740 calcimimetic calindol prevents high phosphate-induced vascular calcification by
741 upregulating matrix GLA protein, Nephron Exp. Nephrol. 122 (2012) 75–82.
742 doi:10.1159/000349935.

743 [46] O. Ivanovski, I.G. Nikolov, N. Joki, A. Caudrillier, O. Phan, R. Mentaverri, J.
744 Maizel, Y. Hamada, T. Nguyen-Khoa, M. Fukagawa, S. Kamel, B. Lacour, T.B.
745 Drüeke, Z.A. Massy, The calcimimetic R-568 retards uremia-enhanced vascular
746 calcification and atherosclerosis in apolipoprotein E deficient (apoE-/-) mice,
747 Atherosclerosis. 205 (2009) 55–62. doi:10.1016/j.atherosclerosis.2008.10.043.
748 [47] A. Bellasi, M. Reiner, F. Pétavy, W. Goodman, J. Floege, P. Raggi, Presence of
749 valvular calcification predicts the response to cinacalcet: data from the
750 ADVANCE study, J. Heart Valve Dis. 22 (2013) 391–399.
751 [48] J. Floege, P. Raggi, G.A. Block, P.U. Torres, B. Csiky, A. Naso, K. Nossuli, M.
752 Moustafa, W.G. Goodman, N. Lopez, G. Downey, B. Dehmel, G.M. Chertow,
753 ADVANCE Study group, Study design and subject baseline characteristics in the
754 ADVANCE Study: effects of cinacalcet on vascular calcification in haemodialysis
755 patients, Nephrol. Dial. Transplant. 25 (2010) 1916–1923.
756 doi:10.1093/ndt/gfp762.
757 [49] P. Raggi, G.M. Chertow, P.U. Torres, B. Csiky, A. Naso, K. Nossuli, M.
758 Moustafa, W.G. Goodman, N. Lopez, G. Downey, B. Dehmel, J. Floege,
759 ADVANCE Study Group, The ADVANCE study: a randomized study to evaluate
760 the effects of cinacalcet plus low-dose vitamin D on vascular calcification in
761 patients on hemodialysis, Nephrol. Dial. Transplant. 26 (2011) 1327–1339.
762 doi:10.1093/ndt/gfq725.
763 [50] G.M. Chertow, R. Correa-Rotter, G.A. Block, T.B. Drueke, J. Floege, W.G.
764 Goodman, C.A. Herzog, Y. Kubo, G.M. London, K.W. Mahaffey, T.-C. Mix, S.M.
765 Moe, D.C. Wheeler, P.S. Parfrey, Baseline characteristics of subjects enrolled in
766 the Evaluation of Cinacalcet HCl Therapy to Lower Cardiovascular Events

(EVOLVE) trial, Nephrol. Dial. Transplant. 27 (2012) 2872–2879. doi:10.1093/ndt/gfr777.

[51] EVOLVE Trial Investigators, G.M. Chertow, G.A. Block, R. Correa-Rotter, T.B. Drüeke, J. Floege, W.G. Goodman, C.A. Herzog, Y. Kubo, G.M. London, K.W. Mahaffey, T.C.H. Mix, S.M. Moe, M.-L. Trotman, D.C. Wheeler, P.S. Parfrey, Effect of cinacalcet on cardiovascular disease in patients undergoing dialysis, N. Engl. J. Med. 367 (2012) 2482–2494. doi:10.1056/NEJMoa1205624.

[52] Z. Ferdous, H. Jo, R.M. Nerem, Differences in valvular and vascular cell responses to strain in osteogenic media, Biomaterials. 32 (2011) 2885–2893. doi:10.1016/j.biomaterials.2011.01.030.

[53] P.M. Taylor, S.P. Allen, M.H. Yacoub, Phenotypic and functional characterization of interstitial cells from human heart valves, pericardium and skin, J. Heart Valve Dis. 9 (2000) 150–158.

[54] A. Roy, N.J. Brand, M.H. Yacoub, Molecular characterization of interstitial cells isolated from human heart valves, J. Heart Valve Dis. 9 (2000) 459–464; discussion 464-465.

[55] J.-H. Chen, C.Y.Y. Yip, E.D. Sone, C.A. Simmons, Identification and characterization of aortic valve mesenchymal progenitor cells with robust osteogenic calcification potential, Am. J. Pathol. 174 (2009) 1109–1119. doi:10.2353/ajpath.2009.080750.

[56] J.A. Benton, H.B. Kern, K.S. Anseth, Substrate properties influence calcification in valvular interstitial cell culture, J. Heart Valve Dis. 17 (2008) 689–699.

Figure legends

Figure 1. Expression and functionality of the CaSR in hVICs. (A and B) Evaluation of CaSR protein expression in hVICs, using immunocytochemistry **(A)** and flow cytometry **(B)**. A control isotype was used as a negative control in both experiments. In the immunocytochemistry results, the scale bars represent 100 µm. **C.** Assessment of CaSR expression by Western blotting. The experiment was performed on protein extracts of hVICs isolated from five different patients. **(D and E)** Western blot assessment of ERK1/2 phosphorylation in hVICs exposed for 15 min to 5 mmol/L Ca^{2+} in the presence of either the calcilytic NPS2143 **(D)** or the calcimimetic R-568 **(E)**. The results correspond to four independent experiments. Error bars correspond to the SEM. ***p<0.001 vs. hVICs exposed to 1.8 mmol/L Ca^{2+}. $p<0.05 vs. hVICs exposed to 5.0 mmol/L Ca^{2+}.

Figure 2. Effects of Ca^{2+} on hVIC calcification and the osteogenic transition. (A) Evaluation (using Alizarin Red staining) of the impact of Ca^{2+} on the development of hVIC mineralization. Alizarin Red staining was performed after 14 days of culture in medium containing 1% FBS and various Ca^{2+} concentrations (1.8, 3.0, 5.0 mmol/L). The results correspond to five independent experiments performed in triplicate. Scale bars: 500 µm. The error bars correspond to the SEM. ***p<0.001 vs. hVICs exposed to 1.8 mmol/L Ca^{2+}. **(B.-F)** Impact of Ca^{2+} (5 mmol/L) on mRNA expression of Bmp2 **(B)**, Runx2 **(C)**, Opn **(D)**, Osx **(E)** and αSMA **(F)**, assessed by qRT-PCR following 1 day (D1), 7 days (D7) and 14 days (D14) of treatment. The results correspond to eight independent experiments performed in duplicate. The error bars correspond to the SEM. *p<0.05, **p<0.01 and ***p<0.001 vs. hVICs exposed to 1.8 mmol/L Ca^{2+} on the same day.

Figure 3. The genetic modulation of CaSR expression dramatically affects Ca^{2+}-induced hVIC mineralization and the osteogenic transition. (A-C) Impact of the overexpression of a functional CaSR (CaSR-WT) on the mineralization and osteogenic transition of hVICs. **(A)** Alizarin Red S staining of hVICs transfected with either EV or a plasmid containing the CaSR-WT and then exposed for 14 days to 1.8 or 5.0 mmol/L Ca^{2+} in medium containing 1% FBS. The results correspond to six independent experiments performed in triplicate. Scale bars: 500 µm. The error bars correspond to the SEM. ***p<0.001 vs. hVICs transfected with the same plasmid and exposed to 1.8 mmol/L Ca^{2+}. $$p<0.01 vs. EV-transfected hVICs exposed to 5.0 mmol/L Ca^{2+}. **(B and C)** The impact of Ca^{2+} (5 mmol/L) on Bmp2 **(B)** and Opn **(C)** mRNA expression in EV- or CaSR-WT-transfected cells, assessed by qRT-PCR following 3 days (D3) of treatment. The results correspond to four independent experiments performed in duplicate. The error bars correspond to the SEM. ***p<0.001 vs. hVICs transfected with the same plasmid and exposed to 1.8 mmol/L Ca^{2+}. $p<0.05 and $$p<0.01 vs. EV-transfected hVICs exposed to 5.0 mmol/L Ca^{2+}. **(D-F)** The impact of CaSR downregulation on the mineralization and osteogenic transition of hVICs. **(D)** Alizarin Red S staining performed on hVICs transfected with either a scrambled (scr) siRNA or the CaSR-siRNA and exposed for 14 days to 1.8 or 5.0 mmol/L of Ca^{2+} in medium containing 1% FBS. The results correspond to eight independent experiments performed in triplicate. Scale bars: 500 µm. The error bars correspond to the SEM. *p<0.05, ***p<0.001 vs. hVICs transfected with the same siRNA and exposed to 1.8 mmol/L Ca^{2+}. $$$p<0.001 vs. hVICs transfected with the scrambled siRNA and exposed to 5.0 mmol/L Ca^{2+}. **(E and F)** Impact of Ca^{2+} (5 mmol/L) on Bmp2 **(E)** and Opn **(F)** mRNA expression in scrambled (scr) or CaSR-siRNA transfected cells, assessed by qRT-PCR following 3 days (D3) of treatment.

The results correspond to four independent experiments performed in duplicate. The error bars correspond to the SEM. *p<0.05 and ***p<0.001 vs. hVICs transfected with the same siRNA and exposed to 1.8 mmol/L Ca^{2+}. $p<0.05 vs. scrambled-transfected hVICs exposed to 5.0 mmol/L Ca^{2+}.

Figure 4. Pharmacological modulation of CaSR activity dramatically affects Ca^{2+}-induced hVIC mineralization and osteogenic transition. (A-C) Impact of the calcimimetic R-568 on the mineralization and osteogenic transition of hVICs. **(A)** Alizarin Red S staining performed on hVICs exposed for 14 days to 1.8 or 5.0 mmol/L of Ca^{2+} in the presence or absence of increasing concentrations of R-568 (0.1, 0.5 and 1 µmol/L) in medium containing 1% FBS. The results correspond to five independent experiments performed in triplicate. Scale bars: 500 µm. The error bars correspond to the SEM. ***p<0.001 vs. hVICs exposed to 1.8 mmol/L Ca^{2+}. $p<0.05 and $$p<0.01 vs. hVICs exposed to 5.0 mmol/L Ca^{2+} in the absence of R-568. **(B and C)** Impact of Ca^{2+} (5 mmol/L) on Bmp2 **(B)** and Opn **(C)** mRNA expression in cells exposed or not to 0.1 µmol/L of R-568, assessed by qRT-PCR following 1 day (D1) of treatment. The results correspond to eight independent experiments performed in duplicate. The error bars correspond to the SEM. ***p<0.001 vs. hVICs exposed to 1.8 mmol/L Ca^{2+}. $$p<0.01 vs. hVICs exposed to 5.0 mmol/L Ca^{2+} in the absence of R-568. **(D-F)** Impact of the calcilytic NPS2143 on the mineralization and osteogenic transition of hVICs. **(D)** Alizarin Red S staining of hVICs exposed for 14 days to 1.8 or 5.0 mmol/L of Ca^{2+} in the presence or absence of increasing concentrations of NPS2143 (0.001, 0.01, and 0.1 µmol/L) in medium containing 1% FBS. The results correspond to nine independent experiments performed in triplicate. Scale bars: 500 µm. The error bars correspond to the SEM. ***p<0.001 vs. hVICs

exposed to 1.8 mmol/L Ca^{2+}. $$p<0.01 vs. hVICs exposed to 5.0 mmol/L Ca^{2+} in the absence of NPS2143. **(E and F)** Impact of Ca^{2+} (5 mmol/L) on Bmp2 **(E)** and Opn **(F)** mRNA expression in cells exposed or not to 0.1 µmol/L of NPS2143, as assessed using qRT-PCR after one day (D1) of treatment. The results correspond to eight independent experiments performed in duplicate. The error bars correspond to the SEM. ***p<0.001 vs. hVICs exposed to 1.8 mmol/L Ca^{2+}. $$p<0.01 vs. hVICs exposed to 5.0 mmol/L Ca^{2+} in the absence of NPS2143.

Figure 5. CaSR expression is elevated in calcified human aortic tricuspid valves. (A) Immunohistologic evaluation of CaSR expression in calcified (C) and non-calcified (NC) human aortic triscuspid valves. Calcification was developed by Alizarin Red staining. A control IgG was used to assess the specificity of the CaSR antibody. Representative images were obtained from four patients. Scale bars: 200 µm. **(B and C)** Western blot evaluation of CaSR expression within calcified (C) and non-calcified (NC) human aortic tricuspid valves. A representative Western blot of samples from four patients is presented in **(B).** The Western blot data obtained from calcified and non-calcified pieces of valve from 12 different donors are quantified in **(C).** The results correspond to 12 independent experiments. The error bars correspond to the SEM. **p<0.01 vs. non-calcified pieces of aortic tricuspid valves.

Figure 1

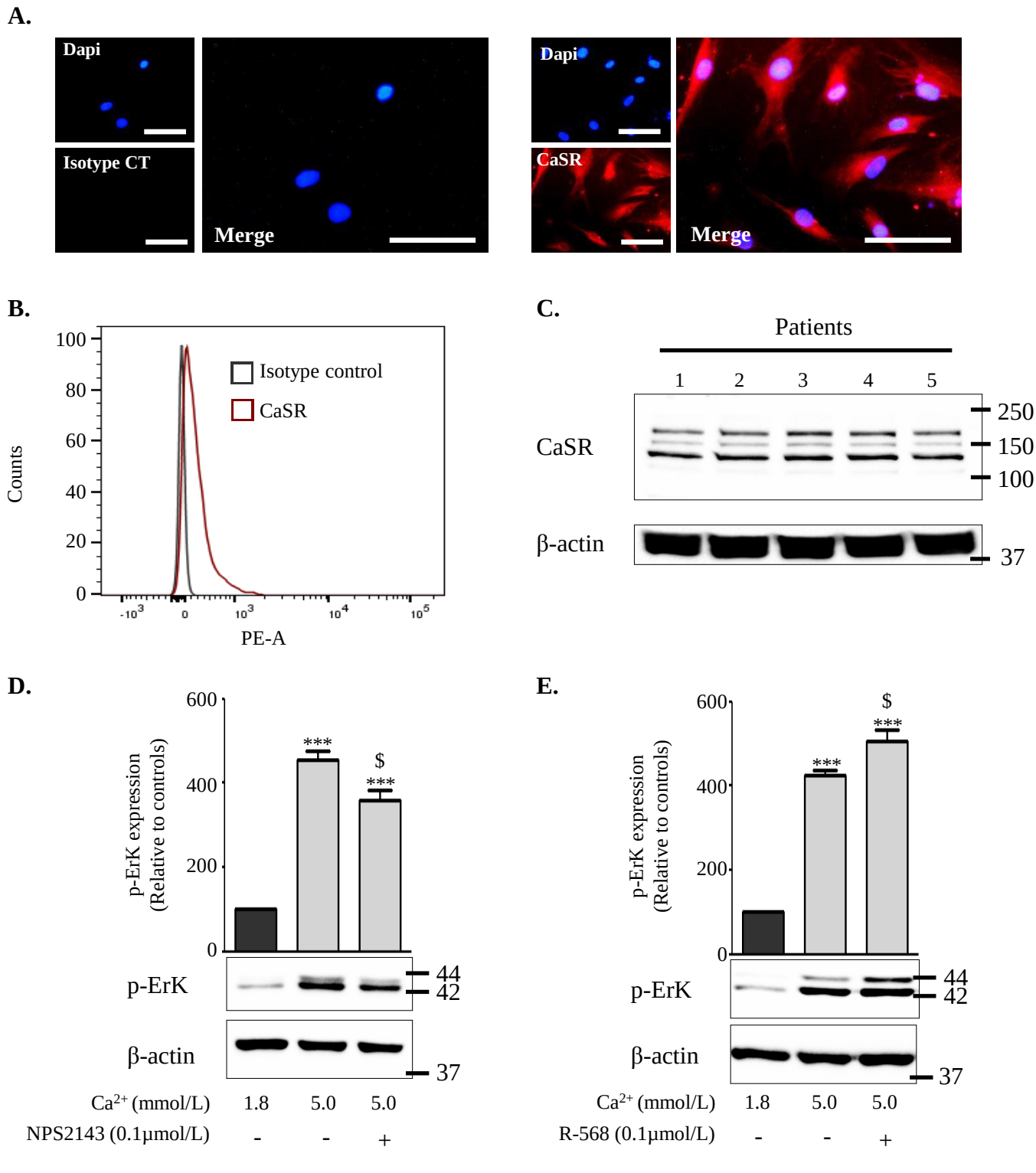
A.
Dapi
Isotype CT
Merge
Dapi
CaSR
Merge
B.
Isotype control
CaSR
Counts
PE-A
C.
Patients
1
2
3
4
5
CaSR
β-actin
250
150
100
37
D.
p-ErK expression (Relative to controls)
***
$
***
p-ErK
β-actin
44
42
37
Ca2+ (mmol/L) 1.8 5.0 5.0
NPS2143 (0.1μmol/L) - - +
E.
p-ErK expression (Relative to controls)
***
$
***
p-ErK
β-actin
44
42
37
Ca2+ (mmol/L) 1.8 5.0 5.0
R-568 (0.1μmol/L) - - +

Figure 2

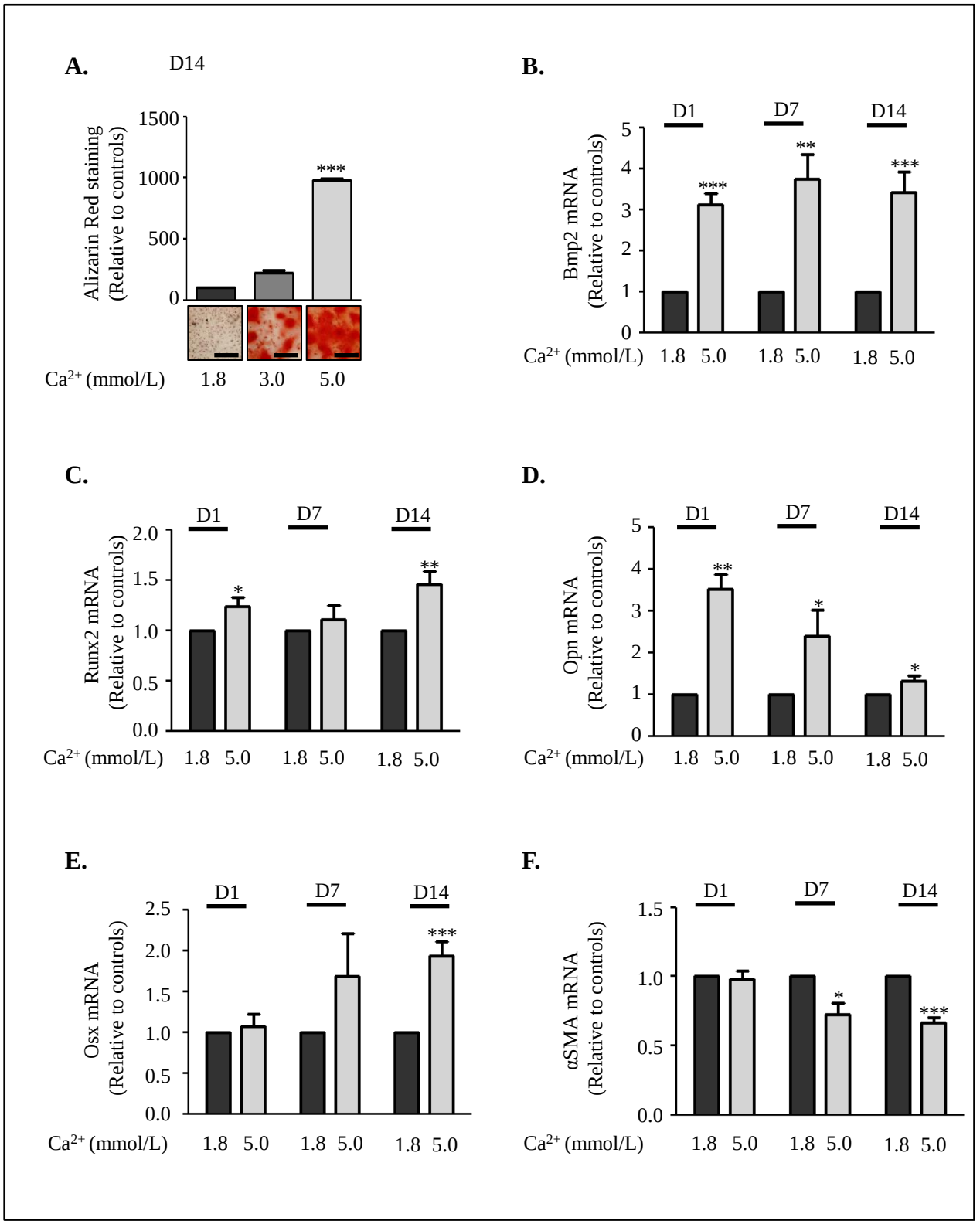
A.
D14
Alizarin Red staining (Relative to controls)
1500
1000
500
0
***
Ca2+ (mmol/L) 1.8 3.0 5.0
B.
D1
D7
D14
Bmp2 mRNA (Relative to controls)
5
4
3
2
1
0
***
**
***
Ca2+ (mmol/L) 1.8 5.0 1.8 5.0 1.8 5.0
C.
D1
D7
D14
Runx2 mRNA (Relative to controls)
2.0
1.5
1.0
0.5
0.0
*
**
Ca2+ (mmol/L) 1.8 5.0 1.8 5.0 1.8 5.0
D.
D1
D7
D14
Opn mRNA (Relative to controls)
5
4
3
2
1
0
**
*
*
Ca2+ (mmol/L) 1.8 5.0 1.8 5.0 1.8 5.0
E.
D1
D7
D14
Osx mRNA (Relative to controls)
2.5
2.0
1.5
1.0
0.5
0.0
***
Ca2+ (mmol/L) 1.8 5.0 1.8 5.0 1.8 5.0
F.
D1
D7
D14
αSMA mRNA (Relative to controls)
1.5
1.0
0.5
0.0
*
***
Ca2+ (mmol/L) 1.8 5.0 1.8 5.0 1.8 5.0

Figure 3

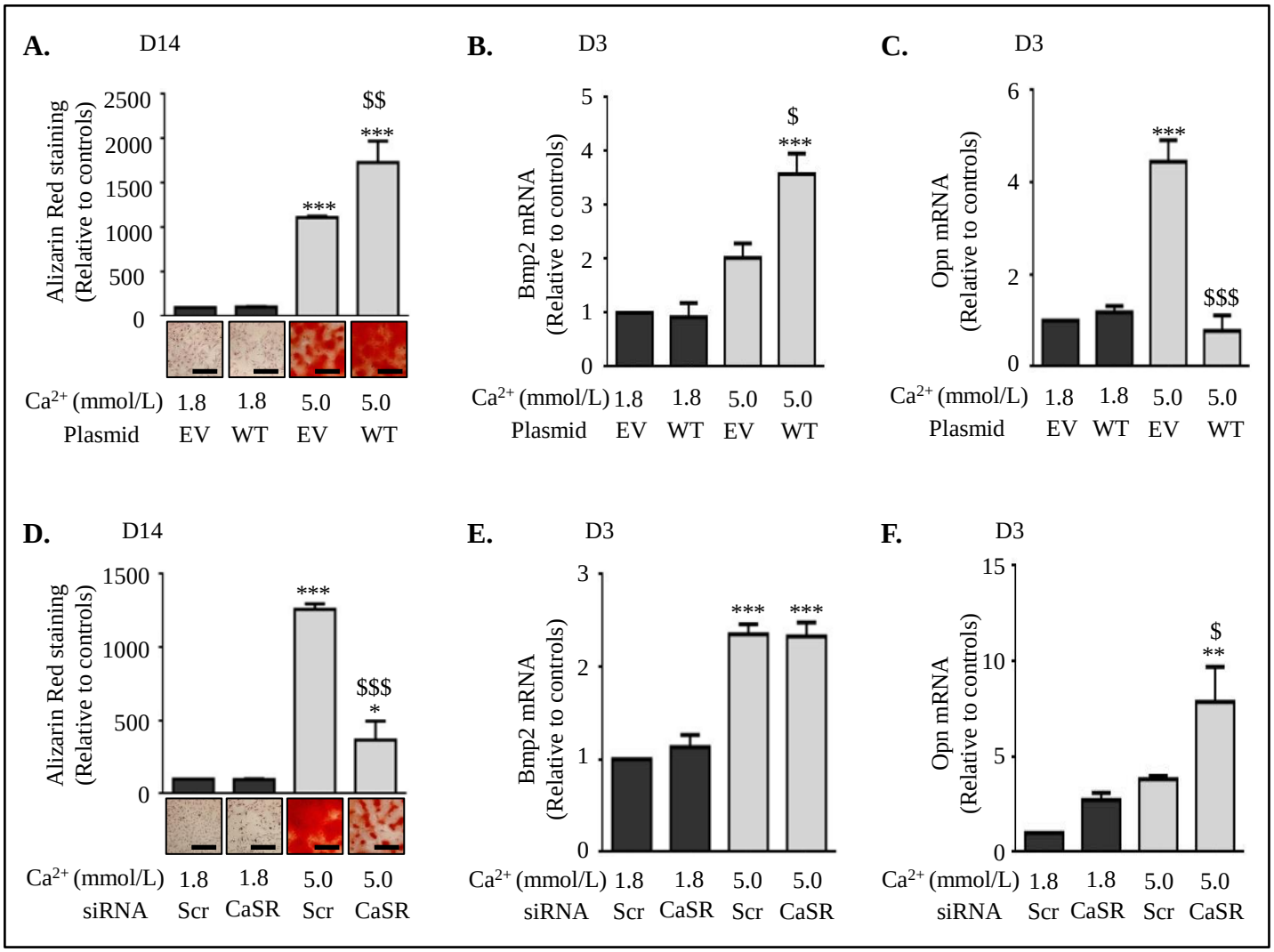
A.
D14
Alizarin Red staining
(Relative to controls)
2500
2000
1500
1000
500
0
$$
***
***
Ca2+ (mmol/L) 1.8 1.8 5.0 5.0
Plasmid EV WT EV WT
B.
D3
Bmp2 mRNA
(Relative to controls)
5
4
3
2
1
0
$
***
Ca2+ (mmol/L) 1.8 1.8 5.0 5.0
Plasmid EV WT EV WT
C.
D3
Opn mRNA
(Relative to controls)
6
4
2
0
***
$$$
Ca2+ (mmol/L) 1.8 1.8 5.0 5.0
Plasmid EV WT EV WT
D.
D14
Alizarin Red staining
(Relative to controls)
1500
1000
500
0
***
$$$
*
Ca2+ (mmol/L) 1.8 1.8 5.0 5.0
siRNA Scr CaSR Scr CaSR
E.
D3
Bmp2 mRNA
(Relative to controls)
3
2
1
0
***
***
Ca2+ (mmol/L) 1.8 1.8 5.0 5.0
siRNA Scr CaSR Scr CaSR
F.
D3
Opn mRNA
(Relative to controls)
15
10
5
0
$
**
Ca2+ (mmol/L) 1.8 1.8 5.0 5.0
siRNA Scr CaSR Scr CaSR

Figure 4

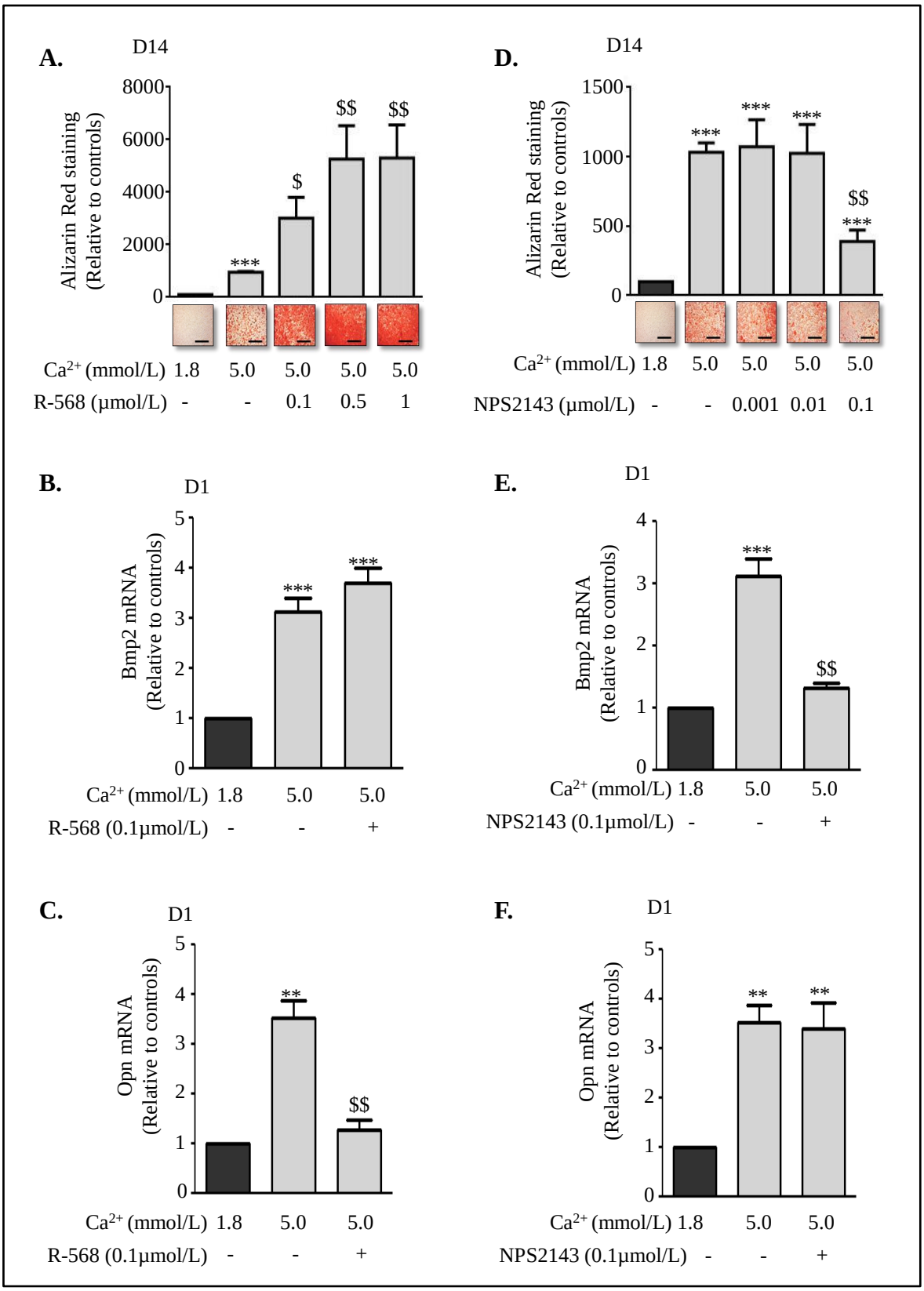
A.
D14
Alizarin Red staining (Relative to controls)
8000
6000
4000
2000
0
***
$
$$
$$
Ca2+ (mmol/L) 1.8 5.0 5.0 5.0 5.0
R-568 (μmol/L) - - 0.1 0.5 1
D.
D14
Alizarin Red staining (Relative to controls)
1500
1000
500
0
***
***
***
$$
***
Ca2+ (mmol/L) 1.8 5.0 5.0 5.0 5.0
NPS2143 (μmol/L) - - 0.001 0.01 0.1
B.
D1
Bmp2 mRNA (Relative to controls)
5
4
3
2
1
0
***
***
Ca2+ (mmol/L) 1.8 5.0 5.0
R-568 (0.1μmol/L) - - +
E.
D1
Bmp2 mRNA (Relative to controls)
4
3
2
1
0
***
$$
Ca2+ (mmol/L) 1.8 5.0 5.0
NPS2143 (0.1μmol/L) - - +
C.
D1
Opn mRNA (Relative to controls)
5
4
3
2
1
0
**
$$
Ca2+ (mmol/L) 1.8 5.0 5.0
R-568 (0.1μmol/L) - - +
F.
D1
Opn mRNA (Relative to controls)
5
4
3
2
1
0
**
**
Ca2+ (mmol/L) 1.8 5.0 5.0
NPS2143 (0.1μmol/L) - - +

Figure 5

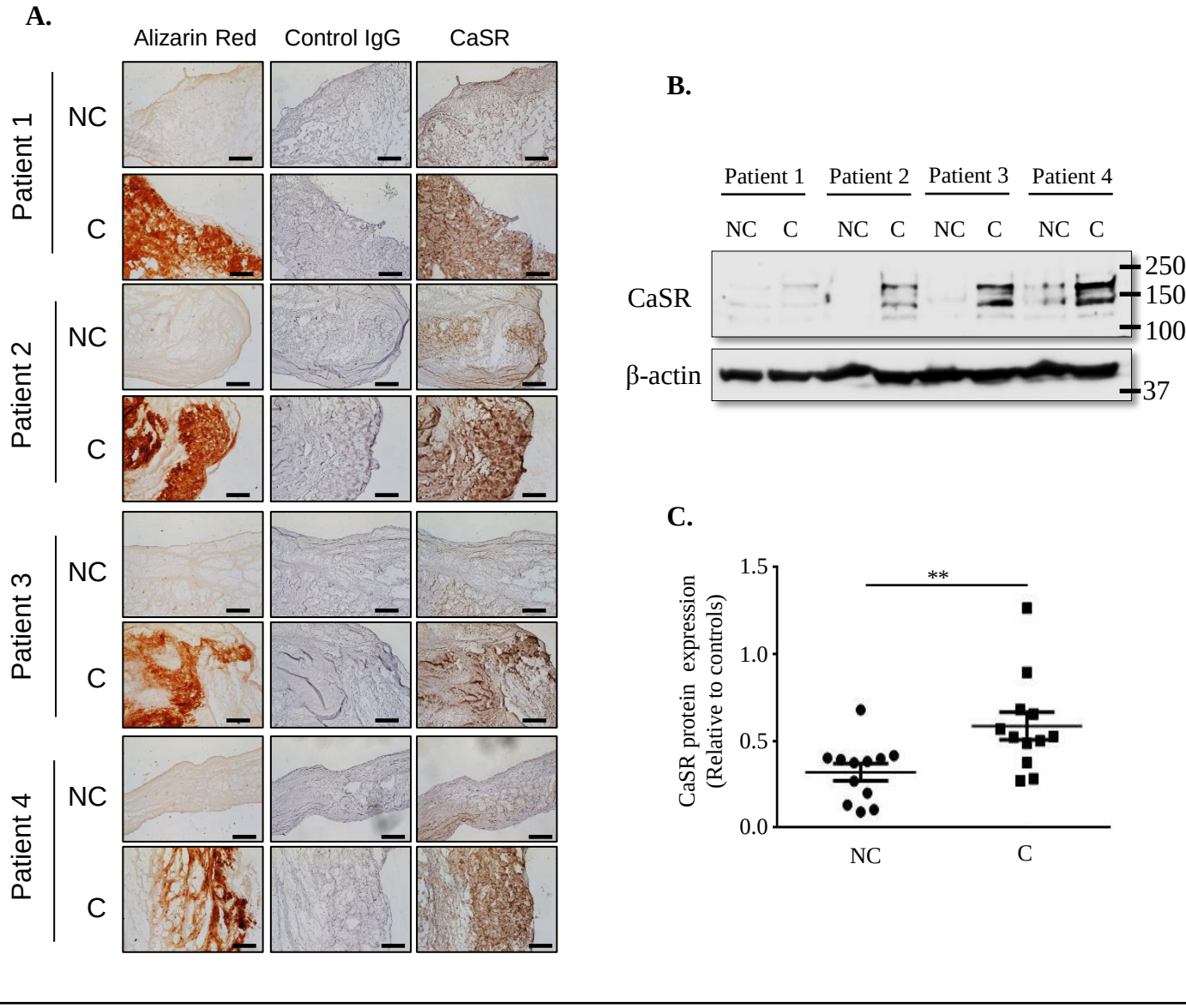
A.
Alizarin Red
Control IgG
CaSR
Patient 1
Patient 2
Patient 3
Patient 4
NC
C
B.
Patient 1
Patient 2
Patient 3
Patient 4
NC C NC C NC C NC C
CaSR
β-actin
250
150
100
37
C.
CaSR protein expression
(Relative to controls)
1.5
1.0
0.5
0.0
**
NC
C